Microenvironmental Effects on the Solvent Quenching Rate in Constrained Tryptophan Derivatives

Hong-Tao Yu, Marco A. Vela, Frank R. Fronczek, Mark L. McLaughlin,* and Mary D. Barkley*

Contribution from the Department of Chemistry, Louisiana State University, Baton Rouge, Louisiana 70803-1804

Received August 25, 1994[⊗]

Abstract: Solvent quenching is one of several environmentally sensitive nonradiative decay pathways available to the indole chromophore. It is characterized by 2−3-fold deuterium isotope effects and strong temperature dependence with frequency factors of $10^{15}-10^{17}$ s^{-1} and activation energies of 11−13 kcal/mol in aqueous solution. The effects of ionization state, proximity of the amino group to the indole ring, and N-methylation of indole nitrogen on the solvent quenching rate were examined in four constrained tryptophan derivatives: 1,2,3,4-tetrahydro-2-carboline, 3-amino-1,2,3,4-tetrahydrocarbazole, 3-amino-1,2,3,4-tetrahydrocarbazole-3-carboxylic acid, and 9-methyl-1,2,3,4-tetrahydro-2-carboline-3-carboxylic acid. The constrained derivatives had at most two ground-state conformations, as determined by X-ray crystallography, molecular mechanics calculations, and ^1H NMR. Fluorescence lifetimes were assigned to ground-state conformations based on relative populations of conformers and amplitudes of fluorescence decays. Solvent quenching rates were determined from the temperature dependence of the fluorescence lifetime. The solvent quenching rate is decreased by protonation of the amino group in all compounds. It is slower in the carboline derivatives, where the amino group is two bonds away from the indole ring, than in the tetrahydrocarbazole derivatives, where the amino group is three bonds away. In the tetrahydrocarbazoles, the solvent quenching rate is slower in the conformer with the ammonium in the pseudoaxial position closer to the indole ring than in the conformer with the ammonium in the pseudoequatorial position pointing away from the ring. These results suggest that the water quenching rate of tryptophans on protein or peptide surfaces is modulated by proximal ammonium groups.

Tryptophan is a superb structural probe in proteins because its fluorescence is highly sensitive to environment.[1,2] However, understanding how emission from the indole chromophore is affected by the many microenvironments possible in proteins is necessary to interpret the fluorescence data. The large solvent effects on the emission maximum are due to the presence of two overlapping electronic transitions with different polarity in the first absorption band, whose relative energy depends on solvent polarity and solvent relaxation.[3] More importantly, the indole chromophore has multiple nonradiative decay pathways that depend on environment. A complex fluorescence decay is usually observed for single tryptophans, whether in proteins,[4−7] peptides,[8−11] or as free amino acid.[12−15] The complex decay kinetics represent multiple ground-state conformers with different microenvironments and consequently different excited-state lifetimes.[13,14,16]

The environmental sensitivity of the fluorescence lifetime τ is mainly due to nonradiative processes

$$\tau^{-1} = k_r + k_{nr} \quad (1)$$

where k_r is the radiative rate and k_{nr} is the overall nonradiative rate. The radiative rate for various indole derivatives determined from quantum yield and lifetime data ranges from 3.5 to 8 × 10^7 s^{-1}.[13,17] The value of k_r is not affected by solvent isotope and temperature, but is increased slightly by a protonated amino group.[9,18] It is a little faster in organic solvents.[17,19] The nonradiative rate of indole includes contributions from several environmentally sensitive pathways: solvent quenching, excited-state proton transfer, and excited-state electron transfer. Solvent quenching refers to the major temperature-dependent nonradiative process that occurs in all indoles in protic solvents and is responsible for the deuterium isotope effect on the fluorescence quantum yield and lifetime of simple indoles.[20] It is character-

[⊗] Abstract published in *Advance ACS Abstracts*, December 1, 1994.

(1) Beechem, J. M.; Brand, L. *Annu. Rev. Biochem.* **1985**, *54*, 43−71.
(2) Eftink, M. R. In *Methods of Biochemical Analysis*; Suelter, C. H., Ed.; John Wiley: New York, 1991; Vol. 35; pp 127−205.
(3) Lami, H.; Glasser, N. *J. Chem. Phys.* **1986**, *84*, 597−604.
(4) DeLauder, W. B.; Wahl, P. *Biochem. Biophys. Res. Commun.* **1971**, *42*, 398−404.
(5) GrinVald, A.; Steinberg, I. Z. *Biochim. Biophys. Acta* **1976**, *427*, 663−678.
(6) Harris, D. L.; Hudson, B. S. *Biochemistry* **1990**, *29*, 5276−5285.
(7) Kim, S.-J.; Chowdhury, F. N.; Stryjewski, W.; Younathan, E. S.; Russo, P. S.; Barkley, M. D. *Biophys. J.* **1993**, *65*, 215−226.
(8) Werner, T. C.; Forster, L. S. *Photochem. Photobiol.* **1979**, *29*, 905−914.
(9) Chang, M. C.; Petrich, J. W.; McDonald, D. B.; Fleming, G. R. *J. Am. Chem. Soc.* **1983**, *105*, 3819−3824.
(10) Chen, R. F.; Knutson, J. R.; Ziffer, H.; Porter, D. *Biochemistry* **1991**, *30*, 5184−5195.
(11) Ross, J. B. A.; Wyssbrod, H. R.; Porter, R. A.; Schwartz, G. P.; Michaels, C. A.; Laws, W. R. *Biochemistry* **1992**, *31*, 1585−1594.
(12) Robbins, R. J.; Fleming, G. R.; Beddard, G. S.; Robinson, G. W.; Thistlethwaite, P. J.; Woolfe, G. J. *J. Am. Chem. Soc.* **1980**, *102*, 6271−6279.
(13) Szabo, A. G.; Rayner, D. M. *J. Am. Chem. Soc.* **1980**, *102*, 554−563.
(14) Petrich, J. W.; Chang, M. C.; McDonald, D. B.; Fleming, G. R. *J. Am. Chem. Soc.* **1983**, *105*, 3824−3832.
(15) Gudgin-Templeton, E. F.; Ware, R. W. *J. Phys. Chem.* **1984**, *88*, 4626−4631.
(16) Donzel, B.; Gauduchon, P.; Wahl, P. *J. Am. Chem. Soc.* **1974**, *96*, 801−808.
(17) Kirby, E. P.; Steiner, R. F. *J. Phys. Chem.* **1970**, *74*, 4480−4490.
(18) Tilstra, L.; Sattler, M. C.; Cherry, W. R.; Barkley, M. D. *J. Am. Chem. Soc.* **1990**, *112*, 9176−9182.
(19) Yu, H.-T.; Colucci, W. J.; McLaughlin, M. L.; Barkley, M. D. *J. Am. Chem. Soc.* **1992**, *114*, 8449−8454.
(20) McMahon, L. P.; Colucci, W. J.; McLaughlin, M. L.; Barkley, M. D. *J. Am. Chem. Soc.* **1992**, *114*, 8442−8448.

0002-7863/95/1517-0348$09.00/0 © 1995 American Chemical Society

ized by strong solvent isotope and temperature dependencies. Intramolecular excited-state proton transfer occurs in tryptophan and tryptamine, where the ammonium group on the side chain initiates proton exchange at the C4 position of indole.[21,22] An analogous intermolecular proton transfer takes place at several aromatic carbons in the presence of exogenous proton donor.[19] Both excited-state proton-transfer reactions are detected in photochemical isotope exchange experiments by NMR or mass spectrometry. They are characterized by strong solvent isotope but weak temperature dependencies. Electron transfer from the excited indole ring to an electrophilic acceptor has been inferred from solute quenching experiments[23,24] and substituent effects.[14,25] It may explain the intramolecular quenching in tryptophan derivatives by carboxylate anion and ester.[14,24,26,27]

Two other well-known nonradiative processes in indoles are intersystem crossing from the first excited singlet state to a triplet state and photoionization to form a solvated electron. The intersystem crossing rate of indole is temperature independent.[28] Tryptophan in proteins and some tryptophan derivatives appear to have two triplet states, suggesting that intersystem crossing rates may depend on environment and perhaps also on temperature.[29,30] Photoionization occurs from a nonrelaxed prefluorescent state[31] and therefore does not affect the fluorescence lifetime, but lowers the fluorescence quantum yield. Lastly, there is no evidence for internal conversion in indoles. The low-temperature luminescence yield of tryptophan[32] and the sum of fluorescence and triplet yields of indole at 1.5 °C[28] are close to unity. Values less than unity can be attributed to photoionization.

Relating the fluorescence lifetime of tryptophan to ground-state conformation has been difficult because both the number and structure of conformers are frequently unknown. Moreover, the multiple nonradiative decay pathways of indole complicate efforts to explain the lifetime differences among conformers in the few cases where it is possible to correlate lifetimes and structures.[11,26] We previously assigned the two fluorescence lifetimes of a constrained tryptophan derivative, 3-carboxy-1,2,3,4-tetrahydro-2-carboline, W(1), as well as its ethyl ester,

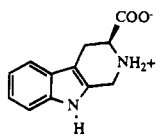

W(1)

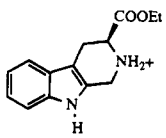

W(1)E

W(1)E, to the two half-chair forms of the partially unsaturated ring.[26] This was achieved by comparing relative amplitudes of fluorescence decays with ground-state populations of conformers determined by molecular mechanics calculations and NMR. The shorter lifetime species has the carboxylate pseudoaxial to the indole ring, whereas the longer lifetime species has the carboxylate pseudoequatorial to the ring. We subsequently showed that the solvent quenching rate depends on the ionization state of the amino group.[20] This paper characterizes the ground- and excited-state properties of a set of constrained tryptophan derivatives that vary the position of the ammonium with respect to the indole ring. The temperature dependence of the fluorescence lifetime is used to determine the rates of individual nonradiative decay processes and to examine their dependence on ground-state structure.

Experimental Section

Synthesis. 1,2,3,4-Tetrahydro-2-carboline, W(1a), was purchased from Aldrich, recrystallized from aqueous ethanol, and sublimed under reduced pressure. Other compounds were synthesized and purified as described below. All compounds were stored in the freezer protected from light. Solutions were made in H_2O and D_2O (Aldrich, >99% D) containing 0.01 M phosphate buffer at the desired pH.

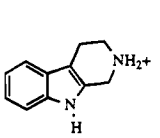

W(1a)

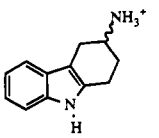

W(1b)

3-Amino-1,2,3,4-tetrahydrocarbazole, W(1b), was prepared according to Borsch et al.[33] The starting ketone, 1,2,3,4-tetrahydrocarbazol-3-one, was obtained from the hydrolysis of its ketal, which was a coupling product of 1,4-cyclohexanedione monoethylene ketal and phenylhydrazine in a typical Fisher indole synthesis.[34] A solution containing 1.4 g (7.6 mmol) of 1,2,3,4-tetrahydrocarbazol-3-one, 5.8 g (75 mmol) of anhydrous ammonium acetate, and 0.34 g (7.2 mmol) of $LiBH_3CN$ in 60 mL of methanol was stirred for 50 h at room temperature in the presence of 5 g of activated molecular sieve (4 Å). The pH of the solution was adjusted to 2 with 6 N HCl, precipitated salt and molecular sieve were removed by filtration, and the solvent was evaporated under vacuum. The residue was dissolved in 20 mL of water. The solution was extracted twice with 20 mL of ether and once with 20 mL of ethyl acetate. The pH of the aqueous phase was raised to 12 with solid KOH; the precipitate was taken up in 20 mL of CH_2Cl_2 and the aqueous solution was extracted with 10 mL of ethyl acetate and 10 mL of CH_2Cl_2. The combined organic phase was dried with sodium sulfate overnight, filtered, and evaporated to dryness. The residue was dissolved in 20 mL of methanol/CH_2Cl_2 (1:5). The free amine was converted to the hydrochloride by bubbling HCl gas through the solution. The pink solid W(1b)·HCl was recrystallized twice from ethanol/ethyl acetate/cyclohexane (1:1:1) to obtain pure white crystals (0.65 g, 38%). Anal. ($C_{12}H_{15}ClN_2$), C, H, N. RP-HPLC showed a single peak at 8.0 min. Column, C18; flow rate, 1 mL/min; gradient, 5% to 80% B. (A) 10% acetonitrile, 5% 2-propanol buffered by 50 mM sodium acetate at pH 6.3, (B) 100% acetonitrile. FAB-MS: ions at *m/z* (relative intensity) 115 (4), 143 (31), 170 (100) $[M - NH_4Cl]^+$, 187 (54) $[M - Cl]^+$, 222 (1) M^+. ^1H NMR (400 MHz, ref to HDO, pD 7): δ 7.52 (d, Ar−H), 7.42 (d, Ar−H), 7.21 (dd, Ar−H), 7.14 (dd, Ar−H), 3.78 (dddd, H_X), 3.23 (dd, H_A), 2.95 (m, Cl−CH_2), 2.82 (dd, H_B), 2.30−2.10 (m, C6-CH_2).

3-Amino-1,2,3,4-tetrahydrocarbazole-3-carboxylic acid, W(2), was prepared by the method of Britten and Lockwood.[35] Starting from commercially available 1,4-cyclohexanedione monoethylene ketal, 8-amino-1,4-dioxaspiro[4,5]decane-8-carboxylic acid precursor was synthesized, which was then coupled with phenylhydrazine. The four-step synthesis resulted in 18% overall yield for W(2). After recrys-

(21) Saito, I.; Sugiyama, H.; Yamamoto, A.; Muramatsu, S.; Matsuura, T. *J. Am. Chem. Soc.* **1984**, *106*, 4286−4287.
(22) Shizuka, H.; Serizawa, M.; Kobayashi, H.; Kameta, K.; Sugiyama, H.; Matsuura, T.; Saito, I. *J. Am. Chem. Soc.* **1988**, *110*, 1726−1732.
(23) Ricci, R. W.; Kilichowski, K. B. *J. Phys. Chem.* **1974**, *78*, 1953−1956.
(24) Ricci, R. W.; Nesta, J. M. *J. Phys. Chem.* **1976**, *80*, 974−980.
(25) Cowgill, R. W. *Biochem. Biophys. Res. Commun.* **1970**, *207*, 556−559.
(26) Colucci, W. J.; Tilstra, L.; Sattler, M. C.; Fronczek, F. R.; Barkley, M. D. *J. Am. Chem. Soc.* **1990**, *112*, 9182−9190.
(27) McMahon, L. P.; Yu, H.-T.; Vela, M. A.; Fronczek, F. R.; Barkley, M. D. *J. Am. Chem. Soc.*, to be submitted for publication.
(28) Klein, R.; Tatischeff, I.; Bazin, M.; Santus, R. *J. Phys. Chem.* **1981**, *85*, 670−677.
(29) Bent, D. V.; Hayon, E. *J. Am. Chem. Soc.* **1975**, *97*, 2612−2619.
(30) Sudhakar, K.; Phillips, C. M.; Williams, S. A.; Vanderkooi, J. M. *Biophys. J.* **1993**, *64*, 1503−1511.
(31) Mialocq, J. C.; Amouyal, E.; Bernas, A.; Grand, D. *J. Phys. Chem.* **1982**, *86*, 3173−3177.
(32) Bishai, F.; Kuntz, E.; Augenstein, L. *Biochim. Biophys. Acta* **1967**, *140*, 381−394.
(33) Borch, R. F.; Bernstein, M. D.; Durst, H. D. *J. Am. Chem. Soc.* **1971**, *93*, 2897−2904.
(34) Vela, M. Ph.D. Thesis, Louisiana State University, 1990.
(35) Britten, A.; Lockwood, G. *J. Chem. Soc., Perkin Trans. 1* **1974**, 1824−1827.

tallizations from hot water, W(2) was obtained as colorless needles: mp 300–302 °C dec, lit.[35] mp 300 °C dec. Anal. ($C_{13}H_{14}N_2O_2$) C, H, N. RP-HPLC showed a single peak at 9.5 min. Column, C18; flow rate, 1 mL/min; gradient, 20–80% B. (A) water with 0.056% trifluoroacetic acid, (B) acetonitrile with 0.056% trifluoroacetic acid. MS: ions at *m/z* (relative intensity) 143 (100), 230 (10) M^+. ^1H NMR (400 MHz, ref to HDO, pD 7): δ 7.48 (2 × d, H-C13 and H-C10), 7.15 (m, H-C11 and H-C12), 3.30 (d, ^2J(HH) = 16.7 Hz, H-C4), 3.08 (d, ^2J(HH) = 16.7 Hz, H-C4), 2.97 (ddd, $^3J_{AA'}$ = 17.8 Hz, H_A), 2.79 (ddd, $^3J_{A'A}$ = 17.8 Hz, $H_{A'}$), 2.41 (ddd, $^3J_{B'B}$ = 14.27 Hz, $H_{B'}$), 2.31 (ddd, $^3J_{BB'}$ = 14.27 Hz, H_B).

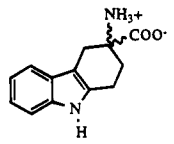

W(2)

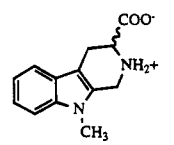

N-Me-W(1)

9-Methyl-1,2,3,4-tetrahydro-2-carboline-3-carboxylic acid, N-Me-W(1). To a solution of 1.0 g (4.67 mmol) of 1-methyl-DL-tryptophan (Aldrich) in 40 mL of 0.1 N NaOH was added 1.14 mL (14.0 mmol) of a 37% formalin solution. The solution was stoppered tightly, placed in an oil bath at 38 °C, and allowed to stir for 48 h. After cooling, the pH was adjusted to 6.5 with 6 N HCl. As the desired pH was approached, the pH was adjusted using 0.1 N NaOH and 0.1 N HCl. An off-white precipitate was collected, crystallized from hot water, and dried (0.11 g, 10%).

X-Ray Diffraction. Pale yellow crystals of W(1a) free amine were grown via slow evaporation of ethanol. Flesh colored crystals of W(2) were recrystallized twice via slow cooling of very dilute boiling pH 6.5 water. Intensity data were collected by ω–2θ scans of variable rate on an Enraf-Nonius CAD4 diffractometer using Cu Kα radiation (λ = 1.541 84 Å) and a graphite monochromator. Crystal data, W(1a): $C_{11}H_{12}N_2$, MW = 172.2; monoclinic space group $P2_1/n$; a = 6.624 (2), b = 10.417(2), c = 13.409(2) Å; β = 92.01(2)°; V = 924.7-(6) Å^3; Z = 4; D_c = 1.237 g cm^{-3}; μ(Cu Kα) = 5.47 cm^{-1}; T = 295 K; crystal size 0.20 × 0.23 × 0.35 mm. A hemisphere of data within 4° < 2θ < 150° was collected. Data reduction included corrections for background, Lorentz, polarization, and absorption. Absorption corrections were based on ψ scans, and the minimum relative transmission coefficient was 94.06%. Equivalent data were merged (R_{int} = 0.016) to yield 1834 unique data, of which 1681 had $I > 3\sigma(I)$ and were used in the refinement. Crystal data, W(2): $C_{13}H_{14}N_2O_2 \cdot 2H_2O$, FW = 266.3; monoclinic space group $P2_1/c$; a = 18.6002(12), b = 6.4530(7), c = 10.752(2) Å; β = 98.100(11)°; V = 1277.6(5) Å^3; Z = 4; D_c = 1.384 g cm^{-3}; μ(Cu Kα) = 8.17 cm^{-1}; T = 296 K; crystal size 0.12 × 0.55 × 0.58 mm. A quadrant of data within 4° < 2θ < 150° was collected. Data reduction included corrections for background, Lorentz, polarization, absorption, and decay. Absorption corrections were based on ψ scans, and the minimum relative transmission coefficient was 66.74%. Intensities declined by 38% during data collection, due to loss of solvent, and a linear correction was applied. Equivalent data were merged (R_{int} = 0.010) to yield 2624 unique data, of which 2452 had $I > 3\sigma(I)$ and were used in the refinement.

The structures were solved by direct methods and refined by full-matrix least-squares based on F with weights $w = \sigma^{-2}(F_o)$, using the Enraf-Nonius SDP programs.[36] Nonhydrogen atoms of W(1a) and W(2) were refined anisotropically including N2 of W(1a), which was disordered into two sites: N2 80% and N2′ 20% occupancy separated by 0.95 Å. All hydrogens of W(1a) and W(2) were located in difference maps and refined isotropically, except for the hydrogen atom on N2′, which was ignored. Secondary extinction coefficients were refined for both structures. At convergence for W(1a): R = 0.044, R_w = 0.058, GOF = 3.078 for 176 variables, extinction = 1.30(2) × 10^{-5}, and the maximum residual density was 0.18 e Å^{-3}. At convergence for W(2): R = 0.046, R_w = 0.065, GOF = 4.014 for 245 variables, extinction = 8.3(3) × 10^{-6}, and the maximum residual density was 0.38 e Å^{-3}. The numbering schemes and perspective views of W(1a) and W(2) are shown in Figures 1 and 2. Final coordinates of W(1a) and W(2) are listed in Tables 1 and 2. Coordinates for hydrogen atoms, bond distances and angles, and anisotropic thermal factors are given in the Supplementary Material.

(36) Frenz, B. A. *Enraf-Nonius Structure Determination Package SDP/VAX V.3.0*; Enraf-Nonius: Delft, The Netherlands, 1985.

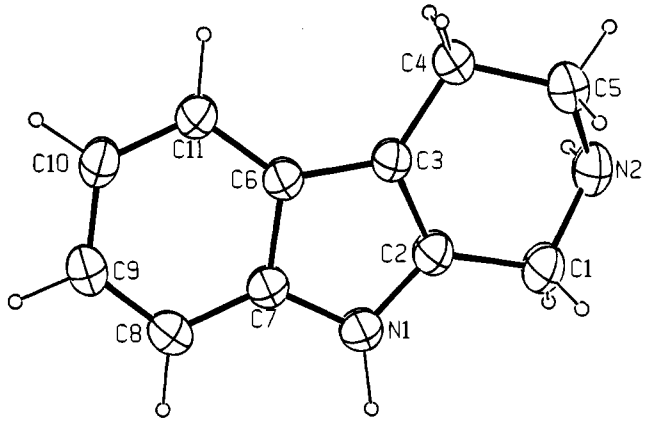

Figure 1. X-ray structure of W(1a) with 40% ellipsoids. The minor site N2′ is not shown.

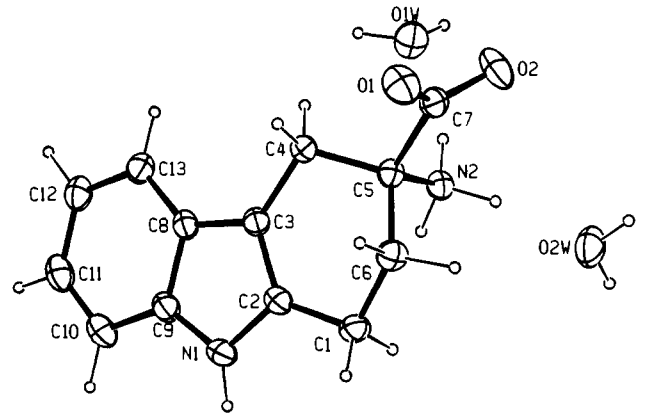

Figure 2. X-ray structure of W(2) with 40% ellipsoids.

Table 1. Coordinates and Equivalent Isotropic Thermal Parameters for W(1a)

atom	x	y	z	B_{eq},[a] Å^2
N1	1.0837(2)	0.296 70(9)	0.332 45(7)	3.98(2)
N2	1.0910(2)	0.63 69(1)	0.239 67(9)	4.07(2)[b]
N2′	1.1724(9)	0.64 61(5)	0.298 8(4)	4.5(1)[c]
C1	1.1909(2)	0.51 31(1)	0.264 64(9)	4.39(2)
C2	1.0534(2)	0.42 64(1)	0.319 17(8)	3.56(2)
C3	0.8820(2)	0.46 55(1)	0.363 39(8)	3.37(2)
C4	0.8163(2)	0.60 35(1)	0.363 4(1)	4.21(2)
C5	0.9786(2)	0.68 77(1)	0.320 5(1)	4.92(3)
C6	0.7961(2)	0.353 70(9)	0.406 98(8)	3.18(2)
C7	0.9277(2)	0.250 0(1)	0.386 89(8)	3.33(2)
C8	0.8899(2)	0.126 0(1)	0.420 21(9)	3.89(2)
C9	0.7209(2)	0.106 0(1)	0.475 14(9)	4.05(2)
C10	0.5889(2)	0.206 3(1)	0.495 71(9)	4.15(2)
C11	0.6243(2)	0.329 4(1)	0.461 74(9)	3.84(2)

[a] $B_{eq} = (8\pi^2/3)\sum_i\sum_j U_{ij}a_i^*a_j^*\mathbf{a}_i\cdot\mathbf{a}_j$. [b] N2 is populated 80%. [c] N2′ is populated 20%.

Molecular Mechanics. Molecular mechanics calculations were done with the MM2 program, modified as described.[26] The dielectric constant of water, ϵ = 78.3, was used in the calculations. Starting coordinates for W(1a) and W(2) were determined from the crystal structures; coordinates of N–Me–W(1) were obtained by replacing the hydrogen on N1 in the crystal structure of W(1) with a methyl group;[26] coordinates for W(1b) were obtained by replacing the ammonium of W(2) with a hydrogen atom and the carboxylate with an ammonium to preserve the definition of torsion angles for the half-chair forms of the cyclohexene ring. Minimization of these initial

Table 2. Coordinates and Equivalent Isotropic Thermal Parameters for W(2)·2H$_2$O

atom	*x*	*y*	*z*	B_{eq},[a] Å^2
O1	0.653 85(5)	0.0349(2)	−0.292 27(8)	3.20(2)
O2	0.557 73(5)	−0.0528(2)	−0.202 44(9)	3.55(2)
N1	0.871 43(6)	−0.2707(2)	0.139 1(1)	2.70(2)
N2	0.630 09(5)	−0.2163(2)	−0.000 57(8)	2.13(2)
C1	0.774 48(7)	−0.3995(2)	−0.034 1(1)	2.50(2)
C2	0.810 22(6)	−0.2371(2)	0.051 9(1)	2.21(2)
C3	0.786 30(6)	−0.0392(2)	0.062 2(1)	2.03(2)
C4	0.722 99(6)	0.0484(2)	−0.023 9(1)	2.04(2)
C5	0.675 82(6)	−0.1254(2)	−0.091 6(1)	1.95(2)
C6	0.722 32(7)	−0.2964(2)	−0.138 5(1)	2.39(2)
C7	0.624 17(7)	−0.0388(2)	−0.205 0(1)	2.22(2)
C8	0.833 56(6)	0.0573(2)	0.163 4(1)	2.13(2)
C9	0.886 64(6)	−0.0927(2)	0.208 3(1)	2.45(2)
C10	0.941 54(7)	−0.0520(3)	0.307 9(1)	3.04(3)
C11	0.941 78(7)	0.1393(3)	0.364 8(1)	3.16(3)
C12	0.888 52(7)	0.2893(2)	0.323 9(1)	2.91(3)
C13	0.834 56(7)	0.2491(2)	0.224 4(1)	2.48(2)
O1W	0.564 14(5)	0.1423(2)	0.089 72(9)	3.25(2)
O2W	0.558 11(6)	−0.5517(2)	−0.106 8(1)	3.84(2)

[a] $B_{eq} = (8\pi^2/3)\sum_i\sum_j U_{ij} a_i^* a_j^* \mathbf{a}_i \cdot \mathbf{a}_j$.

structures yielded the T conformation, which has the carboxylate of W(2) or the amino group of W(1b) in the pseudoequatorial position. Other minimum enthalpy conformational states were explored by driving dihedral angles in the partially unsaturated six-membered rings. Torsional barriers for conformer interconversion were obtained by driving these angles in both directions. Populations were calculated from a Boltzmann distribution at 298 K.

NMR. ^{1}H NMR spectra of W(1b) and W(2) in D$_2$O, pD 7, were recorded on a Bruker AM 400 NMR at room temperature. Resonances in the cyclohexene ring were assigned by decoupling experiments. Assignment of the diastereomeric protons of the AA′BB′ system (Figure 4) of W(2) was based on compounds studied elsewhere. In W(1), 1,2,3,4-tetrahydrocarbazole-3-carboxylic acid [W(1c)], ethyl 1,2,3,4-tetrahydrocarbazole-3-carboxylate [W(1c)E], and 2-amino-1,2-dihydrocyclopenta[*b*]indole-2-carboxylic acid [W(2′)], protons *cis* to carboxylate in the partially unsaturated ring appear to resonate at higher field (smaller chemical shift) compared to protons *trans* to carboxylate.[26,27] In the cyclohexene rings of W(1b), W(1c), and W(1c)E, C1 protons resonate at lower field (larger chemical shift) than C6 protons.[27] In W(2), where H_A on C1 and H_B on C6 are *cis* to carboxylate, we assumed $\delta(H_A) < \delta(H_{A'})$, $\delta(H_B) < \delta(H_{B'})$, and $\delta(H_A), \delta(H_{A'}) > \delta(H_B), \delta(H_{B'})$.

Coupling constants for dihedral angle θ between hydrogens were predicted using the substituted ethane model[26,37]

$$^3J(\theta) = A + B\cos\theta + C\cos 2\theta + \cos\theta\,[(S_1 + S_4)\cos(\theta - 120) + (S_2 + S_3)\cos(\theta + 120)] \quad (2)$$

where the substituent constants S_i were determined from experimental coupling constants for substituted ethanes:

$$S_i = 4(A - {}^3J) \qquad i = 1, 2, 3, 4 \quad (3)$$

Values of ^3J for W(1b) are: H, ethane, 8.0 Hz;[38] $^+NH_3$, *n*-propylamine hydrochloride in D$_2$O, pD 7, 7.53 Hz; C=C, 1-butene, 7.5 Hz;[37] C—C, 2,2-dimethylbutane, 7.56 Hz.[37] Values of ^3J for W(2) are: 2-indolyl-, 2-ethylpyrrole, 7.55 Hz; $^+H_3N(COO^-)C-$, 2-aminobutyric acid in D$_2$O, pD 7, 7.47 Hz. Coupling constants not taken from the literature were measured on a Bruker 200 ACF NMR. Values of $A = 8.0$, $B = -2.7$, and $C = 7.11$ were used in eq 2.[37]

Conformers and populations of W(1b) and W(2) were calculated from experimental coupling constants (Table 5) by solving eqs 4, where

(37) Colucci, W. J.; Jungk, S. J.; Gandour, R. D. *Mag. Reson. Chem.* **1985**, *23*, 335–343.

(38) Lynden-Bell, R. M.; Sheppard, N. *Proc. R. Soc. London A* **1962**, *269*, 385–403.

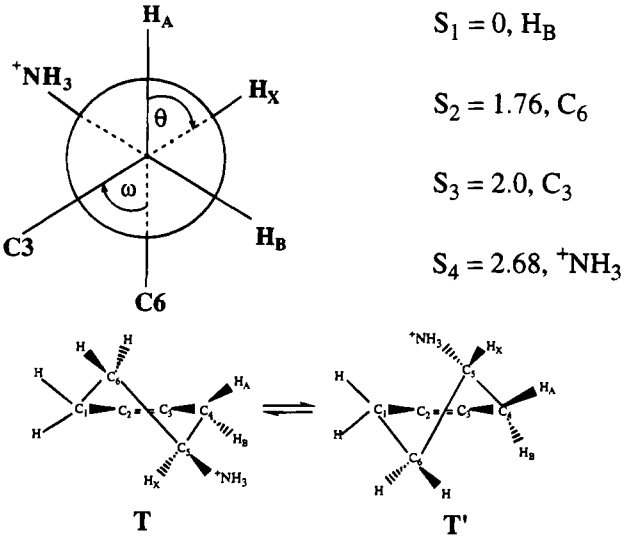

Figure 3. Newman projection of the ABX system in W(1b) and the structure of the T and T′ conformers. The double bond between C2 and C3 represents the indole ring.

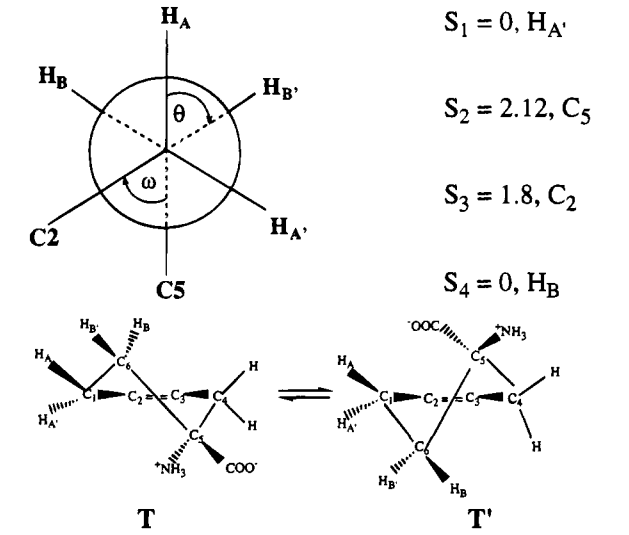

Figure 4. Newman projection of the AA′BB′ system in W(2) and the structure of the T and T′ conformers. The double bond between C2 and C3 represents the indole ring.

θ in eq 2 is expressed in terms of the torsion angle ω for heavy atoms (Figures 3 and 4).

$$^3J_{MN} = \sum_i P_i\, {}^3J(\omega_i) \quad (4a)$$

$$\sum_i P_i = 1 \quad (4b)$$

For the ABX system in W(1b), M = A, B, and N = X. For the AA′BB′ system in W(2), M = A, A′ and N = B, B′. MM2 calculations strongly suggest that W(1b) and W(2) have only two stable conformers, T and T′. Assuming only two conformers, there are three unknowns: two torsion angles, ω_T and $\omega_{T'}$, and the relative population $P_T = 1 - P_{T'}$. For W(1b) the system of equations is underdetermined with two coupling constants. As described elsewhere for W(1), W(1c), and W(1c)E, the torsion angle ω_T of the T conformer was fixed at the MM2 value and eqs 4 were solved for $\omega_{T'}$ and P_T.[26,27] For W(2) the system is overdetermined with four coupling constants. Equations 4 were solved for ω_T, $\omega_{T'}$, and P_T by least squares.

Absorbance. Absorbance was measured on an Aviv 118DS spectrophotometer in 1-cm cells. Temperature was regulated at 25 °C by a circulating water bath. The p*K*s of W(1a), W(2), and N−Me−W(1) were determined from absorbance changes at 280 or 278 nm. Sample absorbance was adjusted to <0.1 at 280 nm for steady-state

fluorescence measurements and <0.2 at 295 nm for time-resolved measurements.

Steady-State and Time-Resolved Fluorescence. Steady-state fluorescence measurements were made on an SLM 8000 spectrofluorometer. Temperature was regulated at 25 °C by a circulating water bath. Fluorescence quantum yields were measured at 280 nm excitation as described before.[20] Tryptophan in water was used as standard with a quantum yield of 0.14.

Fluorescence lifetimes were measured by time-correlated single photon counting on a Photochemical Research Associates instrument with a picosecond dye laser excitation source as described previously.[20] Temperature was regulated by a circulating water bath and monitored with an Omega thermistor. Excitation wavelength was 295 nm. *p*-Terphenyl in ethanol with a single lifetime of 1.06−1.10 ns was used as reference fluorophore. Fluorescence decays for sample and reference fluorophore were acquired contemporaneously in 1024 channels of 27 or 54 ps/channel to about 2.5×10^4 counts in the peak. The data were analyzed by reference deconvolution using the Beechem global program.[39]

Time-resolved emission spectra were acquired at 5- or 10-nm intervals in the region 320- to 400-nm emission wavelength. The data were fitted to a sum of exponentials with amplitudes α_i and lifetimes τ_i. Decay curves acquired at different emission wavelengths were analyzed globally with the lifetimes linked. Decay-associated emission spectra $I_i(\lambda)$ were calculated by combining steady-state and time-resolved data

$$I_i(\lambda) = [\alpha_i(\lambda)\tau_i / \sum_i \alpha_i(\lambda)\tau_i]\, I(\lambda) \tag{5}$$

where $I(\lambda)$ is the steady-state fluorescence intensity and $\alpha_i(\lambda)$ is the amplitude of component i at emission wavelength λ. The data set for W(1b) was also fitted directly to a two-state excited-state reaction as described elsewhere.[27] Ground-state populations P_i were fixed at MM2 and NMR values and conformer lifetimes τ_i and interconversion rates, $k^*_{T-T'}$ and $k^*_{T'-T}$, were linked in the global analysis. The emission spectral contours S_i were not linked. Attempts to equate the emission spectral contours of the two conformers resulted in unphysical values for the interconversion rates.

Radiative rates k_r were calculated from fluorescence quantum yield Φ and lifetime data

$$k_r = \Phi/\tau \tag{6}$$

Lifetimes used in eq 6 were values from monoexponential fits or average lifetimes $\bar{\tau} = \sum_i \alpha_i \tau_i / \sum_i \alpha_i$ from biexponential fits. Nonradiative rates k_{nr} were calculated from eq 1. Photoionization decreases the fluorescence quantum yield by a factor $(1 - \Phi_{pi})$, if the photoionization quantum yield Φ_{pi} is significant. The photoionization yield for aqueous tryptophan in the first absorption band is 0.075;[40] the values for constrained tryptophans are not known. Radiative rates based on fluorescence quantum yields will be underestimated by the factor $(1 - \Phi_{pi})$. The fluorescence lifetime is not affected by photoionization, which occurs in a prefluorescent state. However, underestimating k_r in eq 1 will overestimate k_{nr}.

Fluorescence decays were measured as a function of temperature at one emission wavelength near the emission maximum, except for W(2) anion where decays were measured at three emission wavelengths: 360, 380, and 390 nm. Data were acquired at six to nine temperatures between 5 and 55 °C. Nitrogen gas was flowed through the sample holder to prevent condensation below 20 °C. The temperature dependence of the lifetime is expressed as an Arrhenius factor

$$\tau^{-1} = k_0 + A \exp(-E^*/RT) \tag{7}$$

where k_0 is the temperature-independent rate, A is the frequency factor, E^* is the activation energy, R is the gas constant, and T is the absolute temperature. The Arrhenius parameters k_{0i}, A_i, and E_i^* for component i were linked in global analyses of temperature data in a single solvent.

$$I(t) = \sum_i \alpha_i \exp[-\{k_{0i} + A_i \exp(-E_i^*/RT)\}t] \tag{8}$$

Because previous work showed that k_{0i} and E_i^* are independent of solvent isotope,[20,41] their values were also linked between solvents in global analyses of temperature data sets in H_2O and D_2O. In biexponential fits of the fluorescence decay, the activation energy E_i^* was linked for the two components. The temperature-independent k_{nr}^0 and temperature-dependent k_{si} nonradiative rates are calculated from the Arrhenius parameters

$$k_{nr}^0 = k_0 - k_r \tag{9}$$

$$k_{si} = A \exp(-E^*/RT) \tag{10}$$

Results and Discussion

X-ray Structures. The X-ray structures and atomic labeling of W(1a) and W(2) are shown in Figures 1 and 2. The location and refinement of the three N−H hydrogen atoms in W(2), as well as the essentially equal C−O bond distances of 1.2434(8) and 1.2477(9) Å, demonstrate that this compound exists as the zwitterion in the dihydrate crystal. Its crystallization in a centrosymmetric space group indicates a racemate. There is an extensive hydrogen bonding network in the W(2) dihydrate crystal, involving all three ammonium and all four water hydrogen atoms as donors. The seven independent N···O and O···O distances range from 2.711(1) to 3.026(1) Å, and all angles about H except one (143°) are within 18° of linear. The indole N−H group does not form a hydrogen bond.

The torsion angles of the partially unsaturated six-membered rings of W(1a) and W(2) are compared in Table 3. The cyclohexene ring of W(2) adopts a half-chair or T conformation with the carboxylate occupying a pseudoequatorial position. The conformational disordering seen in the X-ray structure of W(1a) distorts the apparent conformation of the six-membered ring, as the positions of C1 and C5 are averages of unresolved 80% and 20% populated positions, which do not necessarily coincide. Because the thermal parameters of C1 and C5 are not markedly larger than those of C2, C3, and C4, however, it is possible that the apparent distortions are small. The 80% populated N2 position of W(1a) exhibits torsion angles similar to the other half-chair or T′ conformation, whereas the 20% populated N2′ position has torsion angles approximating a flattened twist-boat conformation.

Examination of the intermolecular hydrogen bonding interactions in W(1a) suggest the cause of the disorder. The indole N−H group N1 forms contacts to both positions N2 and N2′ (at $2.5 - x$, $y - 0.5$, $0.5 - z$), with the N···N distance to the 80% position being longer, 2.915(2) versus 2.892(6) Å, but more linear, N-H···N angle 178(2) versus 153(2)°.

Solution Conformation. The conformations of the partially unsaturated six-membered ring were explored by molecular mechanics calculations. Dihedral driver calculations located only two stable half-chair conformations, T and T′, in all the constrained derivatives. W(1b) has the amino group in the pseudoequatorial position in the T conformer. The four compounds have similar torsion angles in both conformations of the six-membered rings (Table 3). The enantiomeric half-chairs of W(1a) have the same enthalpy (Table 4). For the other compounds, the T conformer is enthalpically favored by 0.1 kcal/mol for W(2) to 0.60 kcal/mol for W(1b). The barriers for ring inversion span a 1 kcal/mol range from 4.8 kcal/mol for W(1a) and W(1b) to 5.7 kcal/mol for N−Me−W(1). The relative enthalpies and torsional barrier are not affected by ionization state (data not shown). W(1a) has no chiral center.

(39) Beechem, J. M. *Chem. Phys. Lipids* **1989**, *50*, 237−251.
(40) Bazin, M.; Patterson, L. K.; Santus, R. *J. Phys. Chem.* **1983**, *87*, 189−190.
(41) Lee, J.; Robinson, G. W. *J. Phys. Chem.* **1985**, *89*, 1872−1875.

Table 3. Torsion Angles of T and T′ Conformers Determined by X-ray and MM2

	W(1a)			W(2)			W(1b) MM2		N−Me−W(1) MM2	
		MM2			MM2					
torsion	X-ray[a]	T	T′	X-ray	T	T′	T	T′	T	T′
C3−C4−C5−C7(N)[b]				−164.4	−166.7	−75.9	−165.8	−76.0	−171.2	−73.4
C1−C2−C3−C4	−1.4	−0.1	0.1	−6.5	−0.1	0.1	0.0	0.1	0.36	−0.3
C2−C3−C4−C5	−7.1	20.5	−20.5	18.4	12.2	−20.5	16.2	−13.8	21.0	−22.0
C3−C4−C5−C6(N2)[c]	36.2(−9.2)	−48.3	48.3	−43.2	−39.7	51.5	−47.8	42.0	−48.7	49.5
C4−C5−C6(N2)−C1[c]	−56.2(33.4)	63.1	−63.1	59.0	63.0	−65.7	65.1	−59.1	64.0	−63.6
C2−C1−C6(N2)−C5[c]	42.9(−38.1)	−42.3	42.3	−44.1	−43.3	42.3	−44.6	42.0	−43.4	42.1
C6(N2)−C1−C2−C3[c]	−16.2(24.2)	9.6	−9.6	18.6	15.1	−11.0	14.5	−14.2	15.0	−8.3

[a] Values in parentheses for minor conformation of the carboline ring. [b] N means an amino nitrogen instead of a carbon atom for W(1b). [c] N2 means a carboline nitrogen instead of a carbon atom for W(1a) and N−Me−W(1).

Table 4. Enthalpies, Populations, and Torsional Barriers from MM2 Calculations

	relative enthalpy[a] T′, kcal/mol	P_T,[b] %	$\Delta H^{\ddagger}_{T-T'}$ kcal/mol	$k_{T-T'}$,[c] 10^8 s^{-1}	$k_{T'-T}$,[c] 10^8 s^{-1}
W(1a)	0.0	50	4.8	8.3	8.3
W(1b)	0.60	72	4.8	8.3	16
W(2)	0.10	55	5.2	3.7	4.3
N−Me−W(1)	0.17	60	5.7	1.4	2.3

[a] Enthalpy of T conformer is defined as zero. [b] Calculated from a Boltzmann distribution at 298 K. [c] Estimated from transition-state theory as described in ref 26. The entropy of activation for half-chair inversion is assumed to be zero. A value of 0.4 was used for the transmission coefficient.

Table 5. Torsion Angles and Populations Determined by ^{1}H NMR

	W(1b)	W(2)
coupling constant, Hz		
J_{AX}	8.1	
J_{BX}	5.2	
J_{AB}		6.8
$J_{AB'}$		3.0
$J_{A'B}$		10.8
$J_{A'B'}$		7.5
ω_T, deg	−48	−40
$\omega_{T'}$, deg	33	32
P_T, %	56	68

The two conformers of W(1a) are enantiomers that should differ only in sign of optical rotation; they should have identical fluorescence lifetimes because their structures are mirror images. Methylation of the indole nitrogen of W(1) appears to have little effect on the conformation of the partially unsaturated six-membered ring, though it lowers the relative enthalpy and torsional barrier of T and T′ conformers 0.2−0.3 kcal/mol compared to W(1).[26]

The solution conformations of W(1b) and W(2) were determined by ^{1}H NMR. Two coupling constants were measured for the ABX protons of W(1b) (Figure 3); four coupling constants were measured for the AA′BB′ protons of W(2) (Figure 4). Table 5 lists the coupling constants as well as the torsion angles and populations of T and T′ conformers derived from these coupling constants (see Experimental Section). For W(1b) the torsion angle ω_T of the T conformer was fixed in the calculation at the MM2 value, whereas for W(2) both torsion angles were calculated from NMR data. The NMR value of −40° for ω_T of W(2) concurs with the MM2 value of −43°. However, for both W(1b) and W(2) the NMR and MM2 results for the torsion angle $\omega_{T'}$ of the T′ conformer and the relative populations are only in qualitative agreement. The value of the torsion angle $\omega_{T'}$ is the same in both compounds, with NMR indicating a flatter ring than MM2. While NMR and MM2 identify the T conformer as the major species, the relative population varies from 55% to 70%. The agreement between computed and experimental populations is not as good as it was in W(1).[26] This may be due to deficiencies in the substituted ethane model[37] or to larger errors in deriving coupling constants from the more complicated NMR spectra for the cyclohexene ring.

Absorbance and Steady-State Fluorescence. The absorption spectra of the constrained tryptophan analogues are similar to those of W(1).[18] The spectrum of W(1a) cation is almost identical with the spectrum of W(1) zwitterion with peaks at 270 and 278 nm and a smaller peak at 286 nm. The spectra of W(1b) cation and W(2) zwitterion are less structured with a broad peak at 280 nm and a small peak at 287 nm. At alkaline pH the spectra of the four compounds are all about the same with a smooth peak at 279−281 nm and a shoulder at 285−287 nm. The p*K*s of W(1a), W(2), and N−Me−W(1) at 25 °C were determined by absorbance as before.[18] The p*K* of the ammonium group is 8.4 ± 0.2 for W(1a), 9.1 ± 0.2 for W(2), and 8.6 ± 0.2 for N−Me−W(1). The absorbance change in W(1b) was very small, so the p*K* was estimated from the pH profile of the fluorescence quantum yield. Fluorescence titrations had inflection points in pH 9.8 ± 0.2 for W(1b) and 9.3 ± 0.1 for W(2). These values compare to p*K*s of 8.8 for W(1),[18] 9.8 for W(1b),[42] and 9.4 for tryptophan.[43] In D_2O the p*K* is expected to be about 0.7 unit higher,[44] based on the p*K* shifts in W(1)[20] and tryptophan.[45]

Fluorescence emission maxima λ_{max} and quantum yields of the constrained derivatives are given in Table 6. Deprotonation of the amino group shifts the emission maximum to the red by an amount that depends on proximity to the indole ring. The two carbolines, W(1a) and N−Me−W(1), have the amino group two bonds away, and the two tetrahydrocarbazoles, W(1b) and W(2), have the amino group three bonds away. The emission spectral shift is 14−16 nm for the carbolines, but only 7−10 nm for the tetrahydrocarbazoles. The emission maxima of W(1a) cation and free amine are about the same as W(1) zwitterion and anion, respectively;[18] the maxima of the other compounds lie 4−14 nm to the red of W(1a). Deprotonation of the amino group decreases the fluorescence quantum yield of all the compounds. The quantum yields of both protonated and unprotonated forms are higher in D_2O than in H_2O. This is similar to the behavior of W(1).[20]

Time-Resolved Fluorescence. Fluorescence decays were measured at 25 °C for the protonated and unprotonated forms of the constrained tryptophans in H_2O and D_2O (Table 7). In most cases, the lifetimes of protonated forms are longer than

(42) Eftink, M. R.; Jia, Y.; Hu, D.; Ghiron, C. A. *J. Am. Chem. Soc.*, submitted for publication.
(43) Hermans, J., Jr.; Donovan, J. W.; Scheraga, H. A. *J. Biol. Chem.* **1960**, *235*, 91−93.
(44) Li, N. C.; Tang, P.; Mathur, R. *J. Phys. Chem.* **1961**, *65*, 1074−1076.
(45) Lehrer, S. S. *J. Am. Chem. Soc.* **1970**, *92*, 3459−3462.

Table 6. Steady-State Fluorescence Data in H_2O and D_2O at 25 °C

solvent	λ_{max}, nm	Φ^a	k_r, 10^7 s^{-1}	k_{nr}, 10^7 s^{-1}
		W(1a)		
pH 5.5	347	0.38 ± 0.02	6.8 ± 0.4	11 ± 1
pD 5.5	347	0.42 ± 0.02	6.0 ± 0.3	8.2 ± 0.3
pH 10.5	363	0.21	4.7	18
pD 10.5	364	0.31	4.4	9.7
		W(1b)[b]		
pH 6.0	360	0.24 ± 0.02	5.4 ± 0.3	17
pD 6.0	360	0.35 ± 0.03	4.9 ± 0.3	9.1
pH 11.5	370	0.14	4.9	30
pD 11.5	370	0.24	4.7	15
		W(2)		
pH 6.0	361	0.35 ± 0.02	7.9 ± 0.5	15 ± 1
pD 6.0	361	0.52 ± 0.02	7.4 ± 0.3	6.8 ± 0.3
pH 11	369	0.21	4.7	18
pD 11.5	368	0.31 ± 0.02	4.3 ± 0.3	9.5 ± 0.3
		N−Me−W(1)		
pH 6.0	359	0.52	5.9	5.4
pD 6.0	360	0.58	6.0	4.3
pH 10.5	374	0.45	4.1	5.1
pD 10.5	374	0.54	3.8	3.2

[a] Errors from three to five experiments. [b] Lifetime used to compute k_r from monoexponential fit.

Table 7. Time-Resolved Fluorescence Data in H_2O and D_2O at 25 °C

solvent	α_1 (360 nm)	τ_1, ns	τ_2, ns	χ_r^2
		W(1a)[a]		
pH 5.5		5.61		1.23
pD 5.5		7.06		1.31
pH 10.5		4.46		1.34
pD 10.5		7.10		1.37
		W(1b)[b]		
pH 6.0		4.45		1.51
	−0.02	0.61	4.41	1.04
pD 6.0		7.18		5.59
	−0.02	7.21	7.40	1.24
pH 11.6		2.85		1.15
pD 11.6		5.09		1.23
		W(2)[c]		
pH 6.0		4.73		3.20
	0.18	2.16	4.94	1.30
pD 6.0		7.34		5.71
	0.14	3.74	7.59	1.70
pH 11.0		4.47		3.33
	0.30	3.64	4.80	1.57
pD 11.5		7.30		2.54
	0.37	6.31	7.79	1.55
		N−Me−W(1)[d]		
pH 6.0		8.72		2.30
	0.28	7.73	9.31	1.76
pD 6.0		9.68		2.61
	0.27	7.98	10.32	1.31
pH 10.5		10.89		2.41
pD 10.5		14.35		3.81

[a] 350−400 nm, 10-nm intervals. [b] 335−400 nm, 5-nm intervals for cation; 340−400 nm, 10-nm intervals for free amine. [c] 320−400 nm, 5-nm intervals for zwitterion; 340−400 nm, 5-nm intervals for anion. [d] 330−390 nm, 10-nm intervals.

unprotonated forms, and the lifetimes of both forms are longer in D_2O than in H_2O. W(1a) gave a good fit to a monoexponential function with a lifetime in H_2O of 5.6 ns for the cation and 4.5 ns for the free amine. The lifetime of the cation and free amine increased to 7.1 ns in D_2O. W(1b) cation required a biexponential function to give an acceptable fit. However, the second component has negative amplitude. A negative amplitude in a fluorescence decay is the hallmark of an excited-state reaction. In other tryptophan derivatives the negative amplitude indicates conformer interconversion on the fluorescence time scale.[27,46] Time-resolved emission spectral data were acquired for W(1b) at 5-nm intervals between 335 and 400 nm emission wavelength and were analyzed assuming a two-state excited-state reaction model in the Beechem global program. Ground-state populations of T and T′ conformers were fixed at the values determined by MM2 and NMR, and the lifetimes and interconversion rates of the two conformers were linked in the analysis. The results are given in Table 8. The lifetime is longer for the T′ conformer than the T conformer. This is opposite to the other constrained derivatives we have studied, where the major species associated with the T conformer has the longer lifetime.[18,26,27] In W(1b) the ammonium is closer to the indole ring in the T′ conformer than in the T conformer. Thus, proximity of the ammonium to the indole ring lengthens the fluorescence lifetime. The species-associated emission spectra of the two conformers have similar shapes (not shown). The emission spectral contours S_i are nearly equal with relative values depending slightly on emission wavelength. The fluorescence decay of W(1b) free amine is monoexponential (Table 7).

Table 8. Excited-State Interconversion Model[a]

τ_T(ns)	$\tau_{T'}$(ns)	$k^*_{T-T'}$ (10^8 s^{-1})	$k^*_{T'-T}$ (10^8 s^{-1})	S_T (365 nm)	P_T (%)	χ_r^2
		W(1b), pH 6.0				
2.6 ± 0.6	5.9 ± 1.0	5 ± 1	8 ± 1	0.45	56	1.06
2.7 ± 0.6	6.2 ± 0.4	4 ± 2	8 ± 2	0.43	72	1.06
		W(1b), pD 6.0				
5.8 ± 1.2	8.3 ± 0.6	2 ± 1	5 ± 1	0.43	56	1.29
6.3 ± 0.4	9.2 ± 0.8	2 ± 1	4 ± 2	0.46	72	1.30

[a] Errors from three to five analyses with different initial guesses.

Time-resolved emission spectral data were acquired at 5-nm intervals between 320 and 400 nm for W(2) zwitterion and between 340 and 400 nm for W(2) anion. The data for the zwitterion and the anion in H_2O and D_2O gave good fits to biexponential functions with positive amplitudes (Table 7). The longer lifetime component is the major species, and the average lifetime is slightly longer in the zwitterion than the anion. The relative amplitudes varied with emission wavelength, indicating that the two lifetime components have different spectra. The decay-associated emission spectrum of the shorter lifetime component is shifted 10−20 nm to the blue of the longer lifetime component (Figure 5). In the W(2) zwitterion, the emission maximum occurs at about 345 nm for the shorter lifetime component and 365 nm for the longer lifetime component. A similar spectral association was observed for W(1) zwitterion, where the decay-associated spectrum of the shorter lifetime component was blue-shifted about 10 nm compared to the longer lifetime component.[18] Based on ground-state populations, the major species with longer lifetime is assigned to the T conformer and the minor species with shorter lifetime to the T′ conformer.

The time-resolved emission spectral data for N−Me−W(1) zwitterion gave good fits to biexponential functions with positive amplitudes (Table 7). The lifetimes of the methylated derivative are much longer than the parent compound.[26] Unlike the other constrained derivatives, the lifetimes of N−Me−W(1) increase upon deprotonation of the amino group.

Excited-state conformer inversion rates for W(1b) cation are roughly 2-fold slower in D_2O than H_2O (Table 8). Solvent viscosity is 1.2-fold higher in D_2O than H_2O at 25 °C.[47] Viscosity dependence of conformer interconversion rates is

(46) Willis, K. J.; Szabo, A. G.; Kracjarski, D. T. *Chem. Phys. Lett.* **1991**, *182*, 614−616.
(47) Baker, W. N.; La Mer, V. K. *J. Chem. Phys.* **1935**, *3*, 406−410.

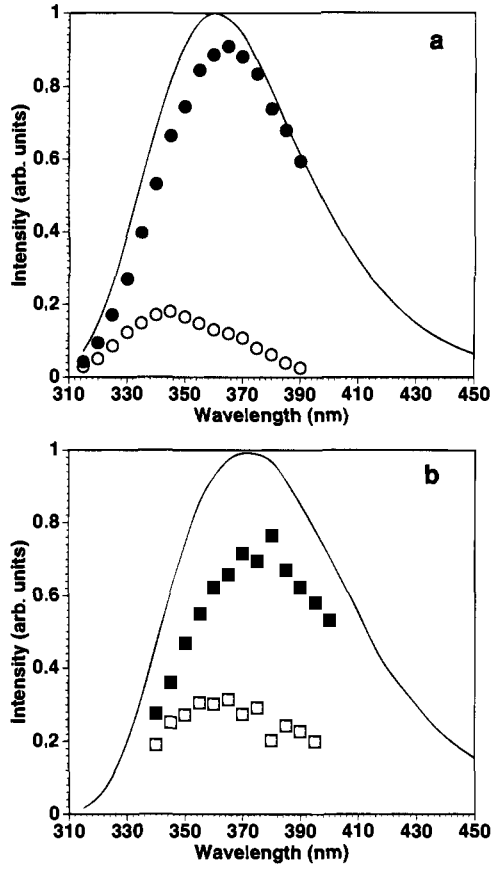

Figure 5. Decay-associated emission spectra of W(2) in D_2O: (a) pD 6.0, (b) pD 11.5. Line denotes the normalized steady-state emission spectrum; (filled symbols) longer lifetime component; (open symbols) shorter lifetime component.

reasonable, because the pendent ammonium on the cyclohexene ring forms hydrogen bonds to water. The excited-state conformer populations can be calculated via the equilibrium constant K^* for conformer inversion in the excited-state

$$T^* \leftrightarrow T'^* \tag{11a}$$

$$K^* = [T'^*]/[T^*] = k^*_{T-T'}/k^*_{T'-T} \tag{11b}$$

The excited-state population of T conformer is 64% in H_2O and 69% in D_2O. The ground-state population is 72% by MM2 and 56% by NMR. Ground-state inversion rates were estimated from transition-state theory using the calculated barrier height (Table 4) as described before:[26,27] $k_{T-T'} = 8.3 \times 10^8\ s^{-1}$ and $k_{T'-T} = 16 \times 10^8\ s^{-1}$. The ground-state values are 2−4 times faster than the excited-state values. As noted previously, the MM2 predicted rates should be considered an upper limit.[26] Barrier heights for conformer interconversion in the excited state can be extracted from the excited-state inversion rates using transition-state theory. Excited-state barriers for W(1b) are estimated to be 5.2 kcal/mol in H_2O, 5.6 kcal/mol in D_2O for the $T^* \rightarrow T'^*$ transition, and 4.7 kcal/mol in H_2O, 5.1 kcal/mol in D_2O for $T'^* \rightarrow T^*$. These values are 0.4−0.9 kcal/mol higher than the ground-state barriers calculated from MM2.

Radiative and nonradiative rates calculated from quantum yield and lifetime data for the constrained derivatives are given in Table 6. The radiative rates k_r of protonated forms are 1.1- to 1.7-fold faster compared to unprotonated forms. Similar increases in k_r upon protonation of the amino group have been reported for tryptophan[9] and W(1).[18] The k_r values are independent of solvent isotope within error. The nonradiative rates are 1.2- to 2.4-fold faster in unprotonated forms than in protonated forms. An increase in k_{nr} upon deprotonation of the amino group was observed in W(1) and attributed to an increase in the solvent quenching rate.[20] The k_{nr} values of all four compounds are faster in H_2O than in D_2O, signifying at least one isotopically sensitive nonradiative process.

Photochemical H−D Exchange. The constrained derivatives W(1a), W(1b), W(2), W(1), and N−Me−W(1) have the ammonium restricted in a six-membered ring. A photochemical isotope exchange experiment was done on W(2) in D_2O, pD 4 as described before.[27] Similar to the results for W(1),[26] no photochemical H−D exchange was detected. Thus, restriction of the ammonium group in either a cyclohexene or carboline ring prevents intramolecular excited-state proton transfer. We can make the same argument for W(1a), W(1b), and N−Me−W(1). Consequently, the isotopically sensitive nonradiative process cannot be attributed to excited-state proton-transfer reactions at aromatic carbons on the indole ring.

Temperature Dependence of Lifetime. The temperature dependence of the fluorescence lifetime is used to separate temperature-dependent and temperature-independent nonradiative rates of indoles.[12,17,20,27,41,48] Fluorescence decays of the constrained tryptophans were acquired as a function of temperature between 5 and 55 °C in H_2O and D_2O. The temperature data sets for each compound in the two solvents were first analyzed as described in the Experimental Section assuming a single exponential term in eq 8. The temperature-independent rate k_0 and activation energy E^* were constrained to be independent of temperature and solvent isotope in the global analyses. Arrhenius parameters are listed in Table 9. The frequency factors of $10^{15}-10^{17}\ s^{-1}$ and activation energies of 10.8−12.6 kcal/mol obtained for the constrained derivatives are similar to the values reported for other indole compounds.[20,41,48] Here too the frequency factors are 2- to 3-fold larger in H_2O than D_2O. The strong solvent isotope effect along with the high frequency factor and activation energy implies a common solvent quenching mechanism for all compounds. The temperature-independent nonradiative rates k^0_{nr} calculated from eq 9 and the temperature-dependent nonradiative rates k_{si} at 298 K calculated from eq 10 are also listed in Table 9. The temperature-independent nonradiative rate k^0_{nr} is insensitive to solvent isotope within error. Deprotonation of the amino group decreases k^0_{nr}. The solvent quenching rate k_{si} depends on solvent isotope through the frequency factor, being 2- to 3-fold faster in H_2O than D_2O. It also depends on ionization state of the amino group. Deprotonation of the amino group increases k_{si} about 2- to 3-fold in all but W(2), where the increase is only about 1.4-fold.

The temperature data sets for W(2) in H_2O and D_2O were also analyzed assuming two components in eq 8 (Table 9). We were unable to resolve two components in the W(1) and N−Me−W(1) temperature data. Because of excited-state conformer interconversion, we did not attempt to resolve two components in the W(1b) data. The global χ_r^2 dropped from 6.5 for the monoexponential fit to 1.5 for the biexponential fit in the W(2) zwitterion and from 5.2 to 1.7 in the anion. The lifetimes at 298 K computed from eq 7 are in excellent agreement with the values obtained from time-resolved emission spectral data (Table 7). The relative amplitudes also agreed well with the values in Table 7, except for W(2) anion in H_2O. Presumably, incorrect amplitudes in these data sets reflect difficulty in resolving two closely spaced decays in the temperature analysis. The temperature-independent k^0_{nr} and

(48) Walker, M. S.; Bednar, T. W.; Lumry, R. In *Molecular Luminescence*; Lim, E. C., Ed.; Benjamin: New York, 1969; pp 135−152.

Table 9. Arrhenius Parameters

	k_0 (10^7 s^{-1})	A (10^{15} s^{-1})	E^* (kcal/mol)	k_{nr}^0 (10^7 s^{-1})	k_{si} (10^7 s^{-1})
			W(1a)		
pH 6	12.8	6.5	11.0	6.0	5.2
pD 6	12.8	3.4	11.0	6.8	2.7
pH 11	9.2	217	12.6	4.5	13
pD 11	9.2	78	12.6	4.8	4.6
			W(1b)		
pH 6	9.6	31	11.4	4.2	13
pD 6	9.6	13	11.4	4.7	6.4
pH 11.6	8.4	71	11.5	2.8	26
pD 11.6	7.7	20	11.2	3.7	12
			N−Me−W(1)		
pH 6	10.1	16	12.5	3.7	1.1
pD 6	10.1	6.3	12.5	3.6	0.5
pH 11	5.7	46	12.4	1.6	3.5
pD 11	5.7	17	12.4	1.9	1.3
			W(1)[a]		
pH 6	13.0	8.1	11.4	5.7	3.4
pD 6	13.0	3.4	11.4	4.8	1.4
pH 11	7.9	21	11.1	2.0	13
pD 11	7.9	7.1	11.1	2.0	4.6
			W(2)[b]		
pH 6	10.1	160	12.4	2.2	13
pD 6	10.1	63	12.4	2.2	5.1
pH 11	6.3	14	10.8	1.6	17
pD 11.5	6.3	6.3	10.8	1.2	7.5
			W(2), τ_1[c]		
pH 6	15.1	20	12.1	7.2	28
pD 6	15.1	13	12.1	7.7	17
pH 11	7.1	28	11.1	2.4	20
pD 11.5	7.1	12	11.1	2.0	8.7
			W(2), τ_2[c]		
pH 6	8.6	9.0	12.1	0.7	12
pD 6	8.6	3.3	12.1	0.7	4.5
pH 11	5.9	19	11.1	1.2	14
pD 11.5	5.9	10	11.1	0.8	7.4

[a] Reference 20. [b] Temperature data set analyzed assuming one exponential term in eq 8. [c] Temperature data set analyzed assuming two exponential terms in eq 8.

temperature-dependent k_{si} rates differ in the two components. Assuming that the radiative rates are the same in both components, k_{nr}^0 and k_{si} are faster in the shorter lifetime component τ_1 than in the longer lifetime component τ_2. The differences in nonradiative rates between conformers are more dramatic in the zwitterion. Thus, it appears that both temperature-independent and temperature-dependent nonradiative processes are faster in the T′ conformer than in the T conformer. The T′ conformer with the faster solvent quenching rate has the amino group in the pseudoequatorial position farther from the indole ring.

Conclusions

In the compounds studied here, the number of ground-state conformers equals the number of excited-state lifetimes. The two enantiomers of W(1a) represent a single conformation with one fluorescence lifetime. W(1b), W(2), and 9−Me−W(1) each have two twist-chair conformers with different lifetimes. The only exceptions are W(1b) free amine and N−Me−W(1) anion, where we were unable to resolve the two lifetimes. These results support the rotamer model of tryptophan photophysics, which attributes excited-state heterogeneity to ground-state heterogeneity. The lifetime difference between conformers is due to the relative proximities of functional groups that affect the rates of nonradiative processes in the indole chromophore.

Solvent quenching is an environmentally sensitive nonradiative process. Beyond the effects of solvent type[6] and isotope,[49,50] three factors in the microenvironment of the indole ring influence the solvent quenching rate k_{si}: (1) ionization state of amino group, (2) proximity of amino group to the ring, and (3) N-methylation of indole nitrogen. Positive charge on the amino group suppresses water quenching in all the constrained tryptophans studied so far. This suppression is more efficient in compounds having an amino group anchored to C2 of indole, such as W(1), W(1a), and N−Me−W(1). Proximity effects of ammonium operate through bond and through space. The water quenching rate is slower when the ammonium group is closer to the indole ring. In the carbolines, the amino group is two bonds away from the ring. Water quenching is slower than it is in the tetrahydrocarbazoles, where the amino group is three bonds away. W(1b) illustrates proximity effects of ammonium through space directly. The T′ conformer, which has the ammonium group in the pseudoaxial position closer to the indole ring, has a longer fluorescence lifetime than the T conformer. This is opposite to other constrained tryptophans, in which the T conformer has the longer lifetime. Individual water quenching rates were measured for the conformers of W(2). Water quenching is slower in the T conformer compared to the T′ conformer. The T conformer of W(2) has the ammonium group in the pseudoaxial position close to the indole ring. Methylation of the indole nitrogen suppresses the water quenching process by 3- to 6-fold in various indole derivatives.[8,50] The water quenching rate is so slow in N−Me−W(1) that changes in k_r instead of k_{si} govern the lifetime dependence on ionization state.

The lifetime difference between conformers in W(1b) zwitterion is attributed to differences in the water quenching rate. However, the temperature data set was analyzed assuming a single lifetime component. The Arrhenius parameters used to calculate the solvent quenching rate represent composite values for the two conformers. The rapid conformer interconversion in W(1b) precluded determination of individual Arrhenius parameters for the two conformers. Conformer inversion during the excited-state lifetime is negligible in W(2), and it was possible to determine Arrhenius parameters for the two lifetime components. This dissects the temperature-independent and temperature-dependent contributions to the nonradiative rate of each conformer. In W(2) zwitterion, the longer lifetime τ_2 of the T conformer is due to two factors: slower temperature-independent nonradiative rate k_{nr}^0 and slower water quenching rate k_{si}. The T conformer has the carboxylate in the pseudoequatorial position pointing away from the indole ring and the ammonium in the pseudoaxial position closer to the ring. In the T′ conformer, the two functional groups swap positions. If electron transfer from excited indole to carboxylate were a quenching mechanism, then the electron transfer rate should be slower in the T conformer where the carboxylate is further from the ring.[26] A temperature-independent electron transfer from excited indole to carboxylate is consistent with a slower temperature-independent nonradiative rate in the T conformer compared to the T′ conformer. The value of k_{nr}^0 was calculated assuming that the radiative rate k_r is the same in both conformers. The slower water quenching rate in the T conformer supports the notion that a proximal ammonium group suppresses this nonradiative process. In W(2) anion, the lifetime difference is smaller than it is in the zwitterion. The longer lifetime of the T conformer is due in larger measure to the temperature-independent nonradiative rate k_{nr}^0, the putative electron transfer rate. The solvent quenching rate is about the same in the two conformers. Presumably, this is also the case

(49) Feitelson, J. *Isr. J. Chem.* **1970**, *8*, 241−252.
(50) Hager, J. W.; Demmer, D. R.; Wallace, S. C. *J. Phys. Chem.* **1987**, *91*, 1375−1382.

for W(1b) free amine, where the water quenching rate is close to the maximal rate for indole derivatives.[27]

The environmental sensitivity of solvent quenching has important implications for tryptophan fluorescence in peptides and proteins. Any tryptophan in an aqueous environment, whether on the surface of proteins or in flexible peptides, is susceptible to solvent quenching. The solvent quenching rate will be modulated by positively charged amino groups and perhaps other positively charged groups as well. Approach of the ϵ-amino group of lysine and the N-terminus within 3−5 Å of the indole ring would slow the solvent quenching rate and lengthen the fluorescence lifetime. On the other hand, if these groups contact the ring in the proper orientation to catalyze excited-state proton transfer, they will shorten the fluorescence lifetime. Depending on the quenching mechanism, ammonium can have opposite effects on tryptophan fluorescence.

Acknowledgment. We thank Professor Maurice R. Eftink for providing the synthetic procedure for W(1b), Mr. Calvin A. Becker for synthesizing 9−Me−W(1), and Mr. Lloyd P. McMahon for assisting with lifetime measurements. This work was supported by NIH Grant GM42101.

Supplementary Material Available: Tables of bond distances, bond angles, torsion angles, coordinates for hydrogen atoms, and anisotropic thermal parameters for W(1a) and W(2) (11 pages). This material is contained in many libraries on microfiche, immediately follows this article in the microfilm version of the journal, and can be ordered from the ACS; see any current masthead page for ordering information.

JA942847Z